

A Novel Copper Cobalt Inorganometallic Cluster. Synthesis, Structure and Bonding Analysis of $\text{Cu}_3\{\mu_2\text{-}(\text{CCHCo}_2(\text{CO})_6)\}_3$

Andrés Vega,^{†,‡,||} Víctor Calvo,^{*,†,‡} Evgenia Spodine,^{*,†,‡} Antonio Zárate,^{‡,§} Víctor Fuenzalida,^{‡,§} and Jean-Yves Saillard^{*,||}

Facultad de Ciencias Químicas y Farmacéuticas, Universidad de Chile, Casilla 233, Santiago, Chile, Facultad de Ciencias Físicas y Matemáticas, Universidad de Chile, Santiago, Chile, and Laboratoire de Chimie du Solide et Inorganique Moléculaire, UMR-CNRS 6511, Institut de Chimie de Rennes, Université de Rennes 1, 35042 Rennes Cedex, France

Received February 11, 2002

The reaction of the organometallic carboxylic acid $\text{HOCCCHCo}_2(\text{CO})_6$ with copper(II) methoxide leads to a new inorganometallic cluster, $\text{Cu}_3\{\mu_2\text{-}(\text{CCHCo}_2(\text{CO})_6)\}_3$. This cluster has a triangular core of copper(I) centers surrounded by three $\text{CCHCo}_2(\text{CO})_6$ fragments. The structure of the cluster has short Cu–Cu and Cu–Co distances (average 2.500 and 2.540 Å, respectively). DFT calculations provide a rationalization of the peculiar bonding in this cluster.

Introduction

A common way to assemble cluster of clusters compounds according to the literature¹ is the exchange of a simple carboxylate salt, like acetate or pivalate, by an organometallic carboxylic acid. This synthetic approach allows the construction of homo and hetero high-nuclearity metal compounds using (mimicking) the well-known carboxylate chemistry.

We are particularly interested in describing the interaction between both metal subsystems (inorganic and organometallic) through an organic bridge. Recently we have prepared and characterized a new carboxylic acid cluster ligand, $\text{HOCCCHCo}_2(\text{CO})_6(\text{Co}_2\text{COOH})$,² which has been successfully used to prepare cluster of clusters compounds of Mo(II).³ Following with the systematic studies about the properties of the cluster of clusters compounds of the ligand Co_2COOH we attempted to synthesize copper(II) complexes with it.

The synthesis of $\text{Cu}_2(\text{OCCO}_2)_4(\text{THF})_2$ by the exchange method, using acetate or trifluoroacetate, is particularly

difficult in terms of product isolation. An alternative route for the preparation of this compound, general to cluster of clusters synthesis, is the reaction of a copper(II) salt with a strongly basic counteranion with the acid ligand Co_2COOH .

This reaction with $\text{B} = \text{OCH}_3$ has been used for the synthesis of cluster of clusters compounds of ligand $\text{HOCCC}_3(\text{CO})_9(\text{Co}_3\text{COOH})$, leading to organometallic carboxylates of Ti, Zr.^{4,5} The reaction of $\text{Zn}(\text{C}_2\text{H}_5)_2$ with the ligand Co_3COOH leads to $\text{Zn}_4\text{O}(\text{OCCO}_3)_6$.^{6,7} It has been described that the organometallic ligand Co_2COOH can be titrated in methanol solution using KOH, and then quantitatively recovered by addition of acid, without any sign of decomposition.² However, a strongly basic medium seems to affect organometallic carboxylates such as Co_3COOH ,^{8–12} and partial decomposition products have been isolated.¹²

Considering all these facts, copper(II) methoxide seemed to be a good option to react with the ligand Co_2COOH , to prepare $\text{Cu}_2(\text{OCCO}_2)_4(\text{THF})_2$ (or another organometallic copper(II) carboxylate). In the present work we show that

* Authors to whom correspondence should be addressed. E-mail: saillard@univ-rennes1.fr (J.-Y.S.); vcalvo@uchile.cl (V.C.); postgrado@uchile.cl (E.S.).

[†] Facultad de Ciencias Químicas y Farmacéuticas, Universidad de Chile.

[‡] Centro para la Investigación Interdisciplinaria Avanzada en Ciencia de los Materiales.

[§] Facultad de Ciencias Físicas y Matemáticas, Universidad de Chile.

^{||} Université de Rennes 1.

(1) Calvo, V.; Fehlner, T. P.; Rheingold, A. L. *Inorg. Chem.* **1996**, *35*, 7289.

(2) Calvo, V.; Vega, A.; Spodine, E. *Inorg. Chim. Acta*, in press.

(3) Calvo, V.; Hernandez, W.; Vega, A.; Spodine, E. Manuscript in preparation.

(4) Lei, X.; Shang, M.; Fehlner, T. P. *Organometallics* **1997**, *16*, 5289.

(5) Lei, X.; Shang, M.; Fehlner, T. P. *Organometallics* **1996**, *15*, 3779.

(6) Cen, W.; Haller, K. J.; Fehlner, T. P. *Inorg. Chem.* **1993**, *32*, 995.

(7) Cen, W.; Haller, K. J.; Fehlner, T. P. *Inorg. Chem.* **1991**, *30*, 3120.

(8) Sturgeon, R.; Olmstead, M.; Schore, N. *Organometallics* **1991**, *10*, 1649.

(9) Lei, X.; Shang, M.; Fehlner, T. P.; Werner, R.; Haase, W.; Hautot, D.; Long, G. J. *Organomet. Chem.* **1997**, *541*, 57.

(10) Lei, X.; Shang, M.; Fehlner, T. P. *Organometallics* **1996**, *15*, 3779.

(11) Calvo, V.; Shang, M.; Yap, G.; Rheingold, A.; Fehlner, T. P. *Polyhedron* **1999**, *18*, 1869.

(12) Calvo, V.; Spodine, E. *Inorg. Chim. Acta* **2001**, *310*, 133.

Table 1. Crystal Data and Structure Refinement Details for $\text{Cu}_3\{\mu_2\text{-(Co}_2)\}_3$

empirical formula	$\text{C}_{24}\text{H}_3\text{Cu}_3\text{Co}_6\text{O}_{18}$
fw	1129.23
cryst syst	triclinic
space group	$P\bar{1}$
$a/\text{\AA}$	9.139(3)
$b/\text{\AA}$	12.077(7)
$c/\text{\AA}$	16.370(6)
α/deg	79.74(4)
β/deg	84.61(3)
γ/deg	78.38(4)
$\text{vol}/\text{\AA}^3$	1738(1)
Z	2
cryst size/mm	$0.30 \times 0.14 \times 0.03$
$D_c/\text{g cm}^{-3}$	2.147
μ/mm^{-1}	4.656
R^a	0.0672
R_w^b	0.1430

$$^a R = \sum ||F_o| - |F_c|| / \sum |F_o|. \quad ^b R_w = [\sum [w(F_o^2 - F_c^2)^2] / \sum [w(F_o^2)^2]]^{1/2}.$$

this reaction scheme unexpectedly leads to the copper(I) cluster $\text{Cu}_3\{\mu_2\text{-(CCHCO}_2\text{(CO)}_6)\}_3$ abbreviated as $\text{Cu}_3\{\mu_2\text{-(Co}_2)\}_3$. We also analyze the electronic structure and bonding of the cluster by means of density functional theory (DFT) calculations and relate these results with the observed decarboxylation reaction.

Experimental Section

Reaction of the Organometallic Ligand Co_2COOH with $\text{Cu}(\text{OCH}_3)_2$. Copper(II) (44 mg) methoxide (0.35 mmol, Aldrich) was dispersed in 20 mL of methanol. A solution of 250 mg of Co_2COOH (0.7 mmol) in 20 mL of dichloromethane was slowly added with stirring. The mixture was allowed to react for 12 h. The solution color went slowly from red to brown. At the end of the reaction time, solvents were completely removed under reduced pressure. Then, 2 mL of $\text{C}_6\text{H}_4\text{Cl}_2$ was used as the extracting solvent. The solution was filtered and allowed to stand at low temperature (-18°C). After a few days, beautiful brown plate-shaped crystals were deposited. These single crystals were identified as $\text{Cu}_3\{\mu_2\text{-(Co}_2)\}_3$ by means of X-ray diffraction.

Anal. Calcd for $\text{Cu}_3\{\mu_2\text{-(CCH}\{\text{Co}_2\text{(CO)}_6\}\}_3$ (%): C, 25.50; H, 0.27; O, 25.50; Cu, 16.88; Co, 31.84. Found (%): C, 25.14; H, 1.51; Cu, 16.3; Co, 31.0.

IR (KBr pellet) cm^{-1} : ν_{CO} 2100(m), 2060(s), 2032(s).

X-ray Analysis. A $0.30 \times 0.14 \times 0.03$ mm dark brown plate was used for structure determination in a Siemens R3m diffractometer. Preliminary scans show acceptable crystal quality. Cell parameters were calculated from least-squares fitting of 25 centered reflections ($7.5^\circ > \theta > 15^\circ$). Data were collected between 3.48° and 50.10° in 2θ at room temperature. Standard reflection showed no crystal decay during data collection. Lorentz and polarization corrections were applied to data set during data reduction, using XDISK.¹³ The structure was solved by direct methods using XS and completed using difference Fourier synthesis. Least squares refinement was carried out until convergence using XL.¹⁴ Hydrogen atoms were located by difference Fourier synthesis and constrained to be at fixed distance of its corresponding pivot atom. This parameter was also refined and was kept constant at the last stages of the refinement. Table 1 shows additional details about structure determination and refinement.

(13) *P3/P4-PC*; Siemens Analytical X-ray Instruments Inc.: Madison, WI, 1991.

(14) Sheldrick, G. M. *SHELXTL/PC*, version 4.2; Siemens Analytical X-ray Instruments Inc.: Madison, WI, 1991.

Photoelectron Spectroscopy. A dichloromethane solution of the cluster $\text{Cu}_3\{\mu_2\text{-(Co}_2)\}_3$ was used to cover the surface of a molybdenum sample holder (which was previously carefully cleaned). A film of the cluster was obtained after the evaporation of the organic solvent, which was then used for measurements. The measurements were performed in a Physical Electronics 1257 system, irradiating with nonmonochromatized Al K α radiation. The angle-resolved system was set at 0° in order to maximize the depth of the collected electrons, thus minimizing surface effects.

Computational Details. (DFT)¹⁵ calculations were carried out using the Amsterdam Density Functional (ADF) program.¹⁶ The Vosko–Wilk–Nusair parametrization¹⁷ was used to treat electron correlation within the local density approximation (LDA). Calculations were also carried out at the nonlocal level, using the corrections to the exchange and correlation energies of Becke¹⁸ and Perdew¹⁹ (BP), respectively. The numerical integration procedure applied for the calculation was developed by te Velde.^{15d} A triple- ζ Slater-type orbital (STO) basis set was used for Cu and Co 3d and 4s. A single- ζ STO was used for Cu and Co 4p. A double- ζ STO basis set was employed for H 1s, C and O 2s and 2p, extended with a single- ζ polarization 2p function for H and 3d for C and O. The frozen core approximation was used to treat core electrons.^{15a} Full geometry optimizations were carried out on each complex using the analytical gradient method implemented by Verluis and Ziegler.²⁰ D_{3h} symmetry was used as a constraint in the geometry optimization of terminal and bridged Cu_3H_3 complexes. The highest possible symmetry for the terminal and bridged $\text{Cu}_3(\text{CH}_3)_3$ systems is C_{3h} or C_{3v} depending on the position of the hydrogen atoms. The 2.3 version of ADF program we used does not recognize C_{3h} symmetry. On the other hand, the C_{3v} symmetry does not allow separation of the in-plane (σ -type) and out-of-plane (π -type) orbitals. Therefore, with the idea of comparing $\text{Cu}_3\{\mu_2\text{-(CH}_3)\}_3$ to $\text{Cu}_3\{\mu_2\text{-(Co}_2)\}_3$, the C_s symmetry was chosen for the $\text{Cu}_3(\text{CH}_3)_3$ models. The optimized geometries were not significantly different from C_{3h} . The same C_s symmetry was considered for cluster $\text{Cu}_3\{\mu_2\text{-(Co}_2)\}_3$ whose optimized structure was also found to be very close to C_{3h} .

Results and Discussion

(a) Molecular Structure. The reaction of the Co_2COOH organometallic carboxylic acid with copper(II) methoxide, as described in the Experimental Section, produces a brown crystalline solid. X-ray diffraction results shows that the structure of the compound corresponds to $\text{Cu}_3\{\mu_2\text{-(Co}_2)\}_3$, as illustrated in Figure 1. Selected bond distances and angles are given in Table 2. The molecule is structurally constituted around an almost equilateral triangular copper central core, which is μ_2 -bridged by three (Co_2) fragments, generated by decarboxylation of the Co_2COOH ligand. The whole molecule is close to C_{3h} symmetry, with a pseudo-mirror plane which contains the Cu_3 triangle and the acetylenic HCC

(15) (a) Baerends, E. J.; Ellis, D. E.; Ros, P. *Chem. Phys.* **1973**, *2*, 41. (b) Baerends, E. J.; Ros, P. *Int. J. Quantum Chem.* **1978**, *S12*, 169. (c) Boerrigter, P. M.; te Velde, G.; Baerends, E. J. *Int. J. Quantum Chem.* **1988**, *33*, 87. (d) Te Velde, G.; Baerends, E. J. *J. Comput. Phys.* **1992**, *99*, 84.

(16) *Amsterdam Density Functional (ADF) program*, version 2.3; Vrije Universiteit: Amsterdam, The Netherlands, 1997.

(17) Vosko, S. D.; Wilk, L.; Nusair, M. *Can. J. Chem.* **1990**, *58*, 1200.

(18) (a) Becke, A. D. *J. Chem. Phys.* **1986**, *84*, 4524. (b) Becke, A. D. *Phys. Rev. A* **1988**, *38*, 2098.

(19) (a) Perdew, J. P. *Phys. Rev. B* **1986**, *33*, 8882. (b) Perdew, J. P. *Phys. Rev. B* **1986**, *34*, 7406.

(20) Verluis, L.; Ziegler, T. *J. Chem. Phys.* **1988**, *88*, 322.

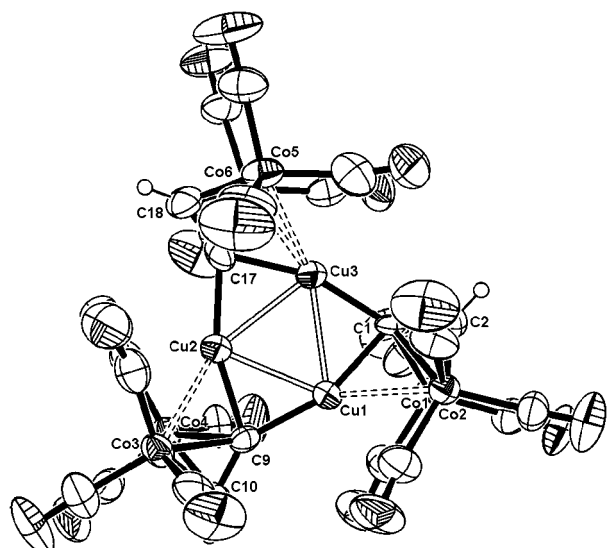


Figure 1. Molecular structure diagram of $\text{Cu}_3\{\mu_2\text{-(CO}_2)\}_3$ with atom-numbering scheme and 33% displacement ellipsoids.

Table 2. Selected Bond Distances (Å) and Angles (deg) for $\text{Cu}_3\{\mu_2\text{-(CO}_2)\}_3$

Cu(1)–Cu(2)	2.494(2)	Cu(1)–Cu(3)	2.499(2)
Cu(2)–Cu(3)	2.508(2)	Cu(1)–Co(1)	2.582(3)
Cu(1)–Co(2)	2.552(2)	Cu(2)–Co(3)	2.588(3)
Cu(2)–Co(4)	2.586(3)	Cu(3)–Co(5)	2.594(2)
Cu(3)–Co(6)	2.599(2)	Cu(1)–C(1)	1.96(1)
Cu(1)–C(9)	1.95(1)	Cu(2)–C(9)	1.94(1)
Cu(2)–C(17)	1.94(1)	Cu(3)–C(1)	1.94(1)
Cu(3)–C(17)	1.96(1)	Co(1)–Co(2)	2.516(2)
Co(3)–Co(4)	2.507(3)	Co(5)–Co(6)	2.508(2)
C(1)–C(2)	1.31(2)	C(9)–C(10)	1.29(2)
C(17)–C(18)	1.31(2)	C(1)–Co(2)	2.09(1)
C(1)–Co(1)	2.14(1)	C(2)–Co(1)	2.00(1)
C(2)–Co(2)	1.99(1)	C(9)–Co(3)	2.09(1)
C(9)–Co(4)	2.10(1)	C(10)–Co(3)	2.00(1)
C(10)–Co(4)	1.96(2)	C(17)–Co(5)	2.08(1)
C(17)–Co(6)	2.11(1)	C(18)–Co(5)	1.95(1)
C(18)–Co(6)	1.97(1)		
Cu(1)–Cu(2)–Cu(3)	59.94(7)	Cu(2)–Cu(1)–Cu(3)	60.31(7)
Cu(1)–Cu(3)–Cu(2)	59.76(7)	C(9)–Cu(1)–C(1)	159.5(5)
C(9)–Cu(2)–C(17)	160.4(5)	C(1)–Cu(3)–C(17)	159.8(4)
Cu(3)–C(1)–Cu(1)	79.7(4)	Cu(2)–C(9)–Cu(1)	79.8(5)
Cu(2)–C(17)–Cu(3)	80.1(4)		

fragments and is perpendicular to the Co–Co bonds. The three (CO₂) fragments are related by a pseudo-C₃ axis. The average distance between carbon atoms in the (CO₂) fragments (1.30 Å) does not statistically deviate from the described value for Co₂COOH (1.29(2) Å).² This is not the case for the C(acetylenic)–Co and Co–Co distances, whose averaged values are 2.040 and 2.510 Å in $\text{Cu}_3\{\mu_2\text{-(CO}_2)\}_3$. Indeed, the measured values for these distances in Co₂COOH are 1.92(2) and 2.486(2) Å, respectively.² The (CO₂)[–] and the phenyl substituted analogue anions have been described coordinated to Fe,²¹ As,²² Re,²³ and Mn.²⁴

- (21) (a) Bruce, M. I.; Duffy, D. N.; Humphrey, M. G. *Aust. J. Chem.* **1986**, *39*, 159. (b) Seyferth, D.; Hoke, J. B.; Rheingold, A. L.; Cowie, M.; Hunter, A. D. *Organometallics* **1988**, *7*, 2163.
 (22) Bird, P. H.; Fraser, A. R. *J. Chem. Soc., Dalton Trans.* **1970**, 681.
 (23) Passynskii, A. A.; Eremenko, I. L.; Nefedov, S. E.; Yanovski, A. I.; Struchkov, Y. T.; Shaposhnikova, A. D.; Stadnichenko, R. A. *Zh. Neorg. Khim.* **1993**, *38*, 455.
 (24) Carriedo, G. A.; Riera, V.; Miguel D.; Lanfredi, A. M. M.; Tiripicchio, A. *J. Organomet. Chem.* **1984**, *272*, C1.

Considering the structure of $\text{Cu}_3\{\mu_2\text{-(CO}_2)\}_3$, there is no doubt that the formal charge of the (CO₂) cluster units is –1. Thus, charge balance indicates that copper corresponds to cuprous ion. This is a surprising result since the copper precursor is a cupric salt (copper(II) methoxide). The Cu(I) oxidation state is confirmed by the XPS spectrum (See Supporting Information). It is dominated by the oxygen and carbon peaks. The copper signal was not detected at the signal/noise ratio of the measurement, indicating that copper is not at the surface. The high-resolution spectrum, recorded with a larger acquisition time, exhibits peaks at 936 and 925 eV, which can be assigned to Cu(I) 2p_{3/2} and 2p_{1/2}, respectively. The most important observation regarding the chemical state of copper is the absence of the shake-up lines around 943 and 962 eV, characteristic of the paramagnetic copper compounds, indicating that copper is in its diamagnetic form Cu(I) or elemental, but not as Cu(II).²⁵ The average Cu(I)···Cu(I) separation is 2.50 Å, a rather short distance when compared with most of the reported values for Cu(I)···Cu(I) distances. For instance, in the dithiolato-bridged Cu₈ cubic clusters, this separation ranges between 2.76 and 2.88 Å.²⁶ In the tetrahedral Cu₄(μ₃-CCR)₄(PR'₃)₄ clusters, the average Cu···Cu separation lies in the range 2.56–2.61 Å.^{27–33} With respect to Cu(I) trinuclear triangular complexes, a search in the Cambridge Structural Database (CSD)³⁴ led to the finding of eight molecular structures, all of them being μ₂- or μ₃-bridged by neutral or ionic ligands.^{27–33} They are listed in Table 3. Their Cu···Cu separations lie in the range 2.38–2.91 Å. Interestingly, the shortest ones are found to be edge-bridged by carbon atoms (2.376 and 2.421 Å in **3** and 2.421 Å in **8**, both compounds presenting isosceles Cu₃ cores with one or two very long Cu···Cu distance). The first theoretical analysis of this type of weak Cu(I)–Cu(I) (d¹⁰–d¹⁰) bonding was made by Hoffmann and Mehrotra.³⁵ They described it as resulting from the mixing of bonding combinations of the vacant Cu 4s and 4p atomic orbitals into the occupied 3d combinations. More recently, Pyykkö stressed the importance of the electron correlation and, for the heavier elements, of relativistic effects in this type of closed-shell/closed-shell bonding.³⁶ Finally, the existence of short Cu···Co nonbonding distances should

- (25) *Handbook of X-Ray Photoelectron Spectroscopy*; Chastain, J. Ed.; Perkin-Elmer Corporation: Eden Prairie, MN, 1992.
 (26) Garland, M. T.; Halet, J.-F.; Saillard, J.-Y. *Inorg. Chem.* **2001**, *40*, 3342.
 (27) Yam, V. W.-W.; Fung, W. K.-M.; Cheung, K.-K. *Organometallics* **1998**, *17*, 3293.
 (28) Niemeyer, M. *Organometallics* **1998**, *17*, 4649.
 (29) Herrmann, E.; Richter, R.; Chau, N. Z. *Anorg. Allg. Chem.* **1997**, *623*, 403.
 (30) Yam, V. W.-W.; Fung, W. K.-M.; Cheung, K.-K. *J. Cluster Sci.* **1999**, *10*, 37.
 (31) Kaluo, T.; Qingchuan, Y.; Jianping, Y.; Youqi, T. *Acta Sci. Nat. Univ. Pekin.* **1988**, *24*, 398.
 (32) Yam, V. W.-W.; Lee, W.-K.; Lai, T.-F. *Organometallics* **1993**, *12*, 2383.
 (33) Aalten, H. L.; van Koten G.; Goubitz, K.; Stam, C. H. *J. Chem. Soc., Chem. Commun.* **1985**, 1252.
 (34) *Cambridge Structural Data Base*, version 5.20; Cambridge Crystallographic Data Center: Cambridge, U.K., 2001.
 (35) Mehrotra, P. K.; Hoffmann, R. *Inorg. Chem.* **1978**, *17*, 2187.
 (36) Pyykkö, P. *Chem. Rev.* **1997**, *97*, 597.

Table 3. Structurally Characterized Trinuclear Ligand Copper(I) Complexes

compd formula	Cu–Cu distances (Å)	ref
$\{\text{Cu}_3\{\mu_3\text{-CCC}_6\text{H}_4\text{-}p\text{-OC}_6\text{H}_5\}\{\mu_3\text{-CCC}_6\text{H}_4\text{-}p\text{-OCH}_3\}\{\mu_2\text{-CH}_2\text{(P(C}_6\text{H}_5)_2)_3\}^+\}$ (1)	2.574, 2.609, 2.621	27
$\{\text{Cu}_3\{\mu_3\text{-CCC}_6\text{H}_4\text{-}p\text{-NO}_2\}\{\mu_3\text{-CCC}_6\text{H}_4\text{-}p\text{-OCH}_3\}\{\mu_2\text{-CH}_2\text{(P(C}_6\text{H}_5)_2)_3\}^+\}$ (2)	2.552, 2.707, 2.758	27
$\text{Cu}_3\{\mu_2\text{-}2',6'\text{-terphenyl}\}\{\mu_2\text{-}\eta_2\text{-}2',6'\text{-terphenyl}\}$ (3)	2.376, 2.421, 2.913	28
$\text{Cu}_3\{\text{N,N-diethyl-N'-diphenoxy thiophosphoryl thioureato}\}_3$ (4)	2.769, 2.773, 2.816	29
$\{\text{Cu}_3\{\mu_3\text{-CCC}_6\text{H}_4\text{-}p\text{-OCH}_3\}_2\{\mu_2\text{-CH}_2\text{(P(C}_6\text{H}_5)_2)_3\}^+\}$ (5)	2.586, 2.613, 2.617	30
$\text{Cu}_3\{\mu_2\text{-SC(Si(CH}_3)_3)\}_3$ (6)	2.640, 2.679, 2.680	31
$\{\text{Cu}_3\{\mu_3\text{-CCC(CH}_3)_3\}\{\mu_3\text{-Cl}\}\{\mu_2\text{-CH}_2\text{(P(C}_6\text{H}_5)_2)_3\}^+\}$ (7)	2.754, 2.791, 2.927	32
$\text{Cu}_3\{\mu_2\text{-OOC}_6\text{H}_5\}_2\{\mu_2\text{-mesityl}\}$ (8)	2.421, 2.888, 2.888	33

also be noted (see Figure 1). The average value for these distances is 2.584 Å.

(b) Theoretical Investigations. To shed some light on the bonding in $\text{Cu}_3\{\mu_2\text{-(CO)}_2\}_3$, and in a more general way of triangular trinuclear Cu(I) clusters, we have undertaken a series of DFT calculations on this compound as well as on other simplified models. If, in the first stage, one neglects the existence of the weak $\text{Co}\cdots\text{Cu}$ contacts in the structure of $\text{Cu}_3\{\mu_2\text{-(CO)}_2\}_3$, the $(\text{CO})_2^- = (\text{CCHCO}_2(\text{CO})_6)^-$ cluster ligands which are bridging the Cu_3^{3+} triangle can be viewed as CR_3^- metalloalkyl anions, with approximately sp^3 carbon atoms bridging the Cu–Cu edges. With a single σ -type occupied frontier orbital, CR_3^- is isolobal to H^- . Therefore, the first simplified model we will consider is Cu_3H_3 .

DFT calculations have been carried out on Cu_3H_3 , at both the LDA and BP levels (see Computational Details). Both terminal and bridging positions of the hydride ligands were considered. The geometry optimizations were carried out under the D_{3h} symmetry constraint. The major computed data are given in Table 4. Calculations of the normal vibration mode frequencies indicate that the bridged structure, $\text{Cu}_3\{\mu_2\text{-H}\}_3$, is a minimum energy, while the one with terminal hydrides is not. Consistently the bridged structure is found to be much more stable than the unbridged one (Table 4). To understand why this structure is the most stable, one has to consider the interaction between the Cu_3^{3+} and H_3^{3-} fragments. Whatever is the hydride bonding mode, the H_3^{3-} fragment has three frontier orbitals of a'_1 and e' symmetry, all of them being occupied. The frontier orbital set of the Cu_3^{3+} triangle results from the interaction of the vacant 4s and 4p AOs of the three metal atoms. The three 4p $_{\pi}$ AOs combine to give rise to a''_2 and e'' combinations which, by symmetry, cannot interact with the frontier orbitals of the H_3^{3-} fragments. The three other Cu AOs constitute the σ -type (in-plane) set and give rise to the following combinations: $2 \times a'_1 + a'_2 + 3 \times e'$. It is not a great deal to predict that, among these nine Cu_3^{3+} 4s/4p combinations, the three lowest ones are of a'_1 and e' symmetry, the former being of major 4s character whereas the latter are mainly made of the σ -type in-plane (π_{σ}) 4p orbitals (see left side of Figure 2). These three frontier orbitals have significant $\text{Cu}\cdots\text{Cu}$ bonding character and are those which are mainly involved in the interaction with the hydrides, as sketched in Figure 2 for $\text{Cu}_3\{\mu_2\text{-H}\}_3$. It should be noted that, since it involves

Table 4. Major Computed Data for the Cu_3X_3 (X = H, CH₃) Models^a

	Cu_3H_3 (terminal ligands) (D_{3h})		$\text{Cu}_3\{\mu_2\text{-H}\}_3$ (D_{3h})		$\text{Cu}_3(\text{CH}_3)_3$ (terminal ligands) (C_3)		$\text{Cu}_3\{\mu_2\text{-(CH}_3)\}_3$ (C_3)	
	BP	LDA	BP	LDA	BP	LDA	BP	LDA
Cu–Cu (Å)	2.744	2.495	2.430	2.364	2.592	2.518	2.412	2.375
Cu–C (Å)					1.960	1.906	2.052–2.170	1.986–2.079
Cu–H (Å)	1.498	1.495	1.688	1.667				
C–H (Å)					1.095	1.099	1.100–1.128	1.100–1.130
$\text{Cu}\cdots\text{H}$ (methyl) (Å)					2.483	2.441	1.997–2.531	1.869–2.493
C–C (Å)								
HOMO–LUMO gap (eV)	0.45	0.30	3.17	3.25	0.54	0.51	3.77	3.67
rel energy (eV)	2.96	3.35	0.00	0.00	1.64	2.57	0.00	0.00
Decomposition of the Bonding Energy								
“steric” interaction energy (eV)		–42.32		–37.92		–39.23		–38.89
orbital interaction energy (eV)								
a'_1		–5.76		–17.76				
a'_2		–0.07		–0.89				
e'		–7.30		–7.84				
a''_1		–0.02		–0.06				
a''_2		–0.06		–0.09				
e''		–0.19		–0.42				
a' (or total σ -type)		$(a'_1 + a'_2 + e' =$ –13.13)		$(a'_1 + a'_2 + e' =$ –26.49)		–15.85		–21.60
a'' (or total π -type)		$(a''_1 + a''_2 + e'' =$ –0.27)		$(a''_1 + a''_2 + e'' =$ –0.57)		–1.51		–2.30
total orbital interaction energy^b (eV)		–13.52		–27.28		–18.03		–24.55
total bonding energy (eV)		–55.85		–65.20		–57.26		–63.45

^a The bonding energy analysis refers to the Cu_3^{3+} and X_3^{3-} fragments. ^b A fitting correction factor has to be added to the sum of the irreducible representation contributions in order to obtain the total orbital interaction energy.

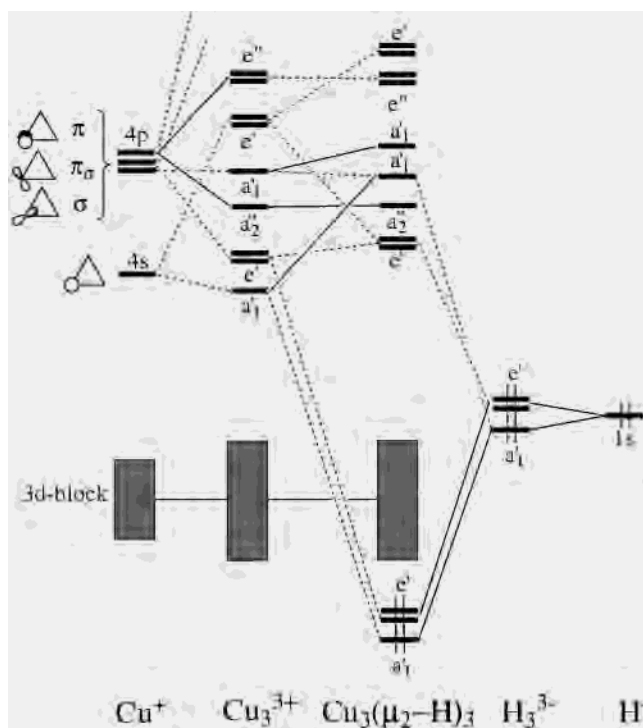


Figure 2. Simplified MO interaction diagram for $\text{Cu}_3\{\mu_2\text{-H}\}_3$.

participation of $\text{Cu}\cdots\text{Cu}$ bonding a'_1 and e' frontier orbitals of Cu_3^{3+} , the bonding with the bridging hydrides tends to strengthen the weak (d^{10})–(d^{10}) bond.

The ADF program provides the opportunity to carry out an analysis of the interaction between the Cu_3^{3+} and H_3^{3-} fragments by using the method of decomposition of the bonding energy between fragments proposed by Ziegler.²⁰ In this method, the bonding energy between the unrelaxed fragments is decomposed into three terms: an electrostatic term, a Pauli repulsion term, and an orbital interaction term. The Pauli repulsion term is generally approximated to the sum of the 4-electron/2-orbital destabilizations, while the orbital interaction term is approximated to the 2-electron/2-orbital stabilizations.³⁷ Moreover, the orbital interaction energy can be decomposed into components associated with the various irreducible representations of the molecule symmetry group. The sum of the electrostatic and Pauli repulsion terms is generally called “steric” interaction energy. In the present case, it is negative due to the strong anion H_3^{3-} /cation Cu_3^{3+} electrostatic interaction. The steric, partial bonding, total bonding, and total interaction energies computed at the LDA level are given in Table 4 for both considered geometries of Cu_3H_3 . From these data, it is clear that what makes the bridged structure the most stable is the a'_1 orbital interaction. This means that the overlap between the a'_1 fragment frontier orbitals is much larger in the bridged structure. This is due to the large 4s character of the a'_1 frontier orbital of Cu^{3+} , as sketched in Figure 3.

The preference for the bridged geometry should be more or less the case for any Cu_3X_3 system in which X is isolobal to H. This is actually what was computed for the C_s (close

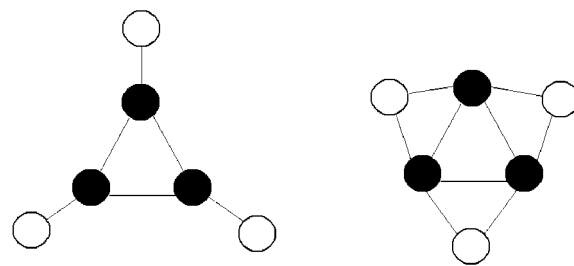


Figure 3. Schematized overlap between the a'_1 frontier orbitals of the Cu_3^{3+} (black circles) and H_3^{3-} (white circles) fragments for the terminal (left) and bridging (right) positions of the hydride ligands.

to D_{3h} , see Computational Details) $\text{Cu}_3\{\text{CH}_3\}_3$ model (Table 4). Due to the lower symmetry considered for this model, it was not possible to decompose the bonding energy in a'_1 and e' components. However, examination of the frontier orbital populations indicates that, as for the Cu_3H_3 system, the energy difference between both considered geometries originates from the a'_1 interaction. Nevertheless, it is possible to decompose the bonding energy into its in-plane (σ -type) and out-of-plane (π -type) components. Methyl is a weak π -donor substituent through its out-of-plane $\sigma(\text{CH})$ bonds.³⁸ This is exemplified by the (weak) a'' component of the bonding energy in $\text{Cu}_3\{\text{CH}_3\}_3$. In the bridged structure, this value, -2.30 eV, is much larger than the corresponding one found for $\text{Cu}_3\{\mu_2\text{-H}\}_3$ (-0.57 eV) which results from the very weak participation of the hydrogen 2p polarization functions. Clearly, the π -type bonding energy computed for $\text{Cu}_3\{\text{CH}_3\}_3$ results from some participation of the out-of-plane $\sigma(\text{CH})$ orbitals. This is supported by an examination of the fragment orbital populations: in $\text{Cu}_3\{\mu_2\text{-(CH}_3)\}_3$, 0.13 electrons are donated by the occupied $\sigma(\text{CH})$ orbitals into the vacant a''_2 and e'' $4p_\pi$ combinations of Cu_3^{3+} . Some in-plane $\text{Cu}\cdots\text{H}$ agostic interaction can also be noticed from the corresponding interatomic distances (Table 4). Finally, it should be noted that the optimized $\text{Cu}\cdots\text{Cu}$ distances of $\text{Cu}_3\{\mu_2\text{-(CH}_3)\}_3$ are not that much different from those which are bridged by carbon atoms in the compounds **3** and **8** of Table 3.

We move now to $\text{Cu}_3\{\mu_2\text{-(CO}_2)\}_3$ which we have optimized in C_s symmetry (see Computational Details). The major computed data are given in Table 5. As is often the case for clusters of transition metals in low oxidation state, the generalized gradient approximation (BP) calculations overestimate the metal–metal bond distances, while the agreement with experimental distances is better at the LDA level.²⁶ Nevertheless, even at the LDA level, the average $\text{Cu}\cdots\text{Cu}$ separation is 0.095 Å larger than the experimental one. Besides that, there is a general good agreement between the computed and experimental structures. The decomposition of the LDA bonding energy between the Cu_3^{3+} and $\{(\text{CO}_2)_3\}^{3-}$ fragments indicates that the σ -type orbital contribution is about the same as in $\text{Cu}_3\{\mu_2\text{-(CH}_3)\}_3$, whereas the π -type contribution is much larger (Table 5). Analysis of the fragment orbital population indicates that only three orbitals of the $\{(\text{CO}_2)_3\}^{3-}$ fragment, of a a''_2 and e'' pseudosymmetry, are involved in the π -type interaction. They are the highest

(37) Landrum, G. A.; Goldberg, H.; Hoffmann, R. *J. Chem. Soc., Dalton Trans.* **1997**, 3605.

(38) Libit, L.; Hoffmann, R. *J. Am. Chem. Soc.* **1974**, *96*, 1370.

Table 5. Major Computed Data for $\text{Cu}_3\{\mu_2\text{-}(\text{CCHCo}_2(\text{CO})_6)\}_3^a$

	$\text{Cu}_3\{\mu_2\text{-}(\text{CCHCo}_2(\text{CO})_6)\}_3$ (C_s)	
	BP	LDA
Cu–Cu (Å)	2.636	2.595
Cu–Co (Å)	2.658	2.520
Co–Co (Å)	2.549	2.472
Cu–C (Å)	1.997	1.955
Co–C(CCH frag) (Å)	2.030	2.027
C(ac)–C(ac) (Å)	1.336	1.329
Decomposition of the Bonding Energy		
“steric” interaction energy (eV)		–24.86
orbital interaction energy (eV)		
a' (σ -type)		–21.35
a'' (π -type)		–8.34
total orbital interaction energy (eV) ^b		–29.96
total bonding energy (eV)		–54.82

^a Distances are averaged. The bonding energy analysis refers to the Cu_3^{3+} and $(\text{CCHCo}_2(\text{CO})_6)_3^{3-}$ fragments. ^b A fitting correction factor has to be added to the sum of the irreducible representation contributions in order to obtain the total orbital interaction energy.

occupied π -type orbitals of the fragment. There is a donation of 0.59 electron of these orbitals into the vacant a''_2 and e'' levels of the Cu_3^{3+} fragment. This donation is much larger than the corresponding one in $\text{Cu}_3(\mu_2\text{-CH}_3)_3$. The question which arises, then, is the nature of this ligand–Cu π -type donation. Is it acting solely through the Cu–C bond, as in $\text{Cu}_3(\mu_2\text{-CH}_3)_3$, or is there in addition some direct $\text{Co}\cdots\text{Cu}$ donation? Analysis of the involved orbitals of a''_2 and e'' pseudosymmetry of the $\{(\text{Co}_2)\}_3^{3-}$ fragment indicates a large metallic character ($\sim 70\%$ on the Co atoms) and a small participation ($\sim 10\%$) of the bridging carbon atom. These orbitals are in fact antisymmetrical combinations of so-called “ t_{2g} ” lone pairs of the Co centers. This indicates that the largest part of the ligand–Cu π -type interaction goes through the $\text{Co}\cdots\text{Cu}$ contacts. Although this cannot be clearly determined because of the low C_s symmetry considered, it is likely that symmetrical (i.e., a') combinations of “ t_{2g} ” lone pairs are also somewhat interacting with σ -type accepting orbitals of the Cu_3^{3+} fragment through the $\text{Co}\cdots\text{Cu}$ contacts.

Despite the similarity of the σ -type components of the orbital interaction energy in $\text{Cu}_3\{\mu_2\text{-}(\text{Co}_2)\}_3$ and $\text{Cu}_3(\mu_2\text{-CH}_3)_3$, the optimized $\text{Cu}\cdots\text{Cu}$ separation is $\sim 9\%$ larger in the former. This suggests that ligand size and steric effects may also be important in determining the length of this weak $d^{10}\text{--}d^{10}$ bond with which a very soft attractive potential is associated.^{26,35} As a matter of fact, the “steric” interaction energies of $\text{Cu}_3\{\mu_2\text{-}(\text{Co}_2)\}_3$ and $\text{Cu}_3\{\mu_2\text{-}(\text{CH}_3)\}_3$ are very different (Tables 4 and 5).

(c) Decarboxylation of Co_2COOH . The obtainment of $\text{Cu}_3\{\mu_2\text{-}(\text{Co}_2)\}_3$ as a reaction product from its Cu(II) precursor leads necessarily to the conclusion that two processes have occurred during reaction: the reduction of Cu(II) to Cu(I) and the decarboxylation of organometallic ligand Co_2COOH to the $(\text{Co}_2)^-$ fragment. Both processes can occur sequentially, or they can be coupled. Literature shows that cluster of clusters compounds such as $\text{Cu}_2(\text{CO}_3)_4(\text{THF})_2$ decompose with deposition of metallic copper mirrors when solutions of the compound are exposed for a long time to room temperature or light.³⁹ In this way, it is not surprising that

under the appropriate conditions (i.e., solvent) the Co_2COOH ligand becomes oxidized by the cupric ion, generating cuprous ion in the reaction media. This process necessary leads to the generation of higher oxidation states of cobalt in the reaction bulk. Besides, the ability of cuprous ion to promote decarboxylation of some activated carboxylic acids (malonic^{40,41} derivatives, phenylacetic^{42,43} derivatives, and cyanoacetic acid⁴⁴) has been reported. It has been shown that an organometallic Cu(I) molecule acts as an intermediate in the reaction path. The stability of this organocuprous intermediate plays a key role, allowing or not allowing the decarboxylation reaction. In this way the reaction between Cu(II) methoxide and Co_2COOH probably proceeds in two steps. A first step generates cuprous ion from reduction of Cu(II) by the organocarboxylic acid Co_2COOH , which in a second step promotes the decarboxylation of the nonoxidized ligand, leading to $\text{Cu}_3\{\mu_2\text{-}(\text{Co}_2)\}_3$. In the reaction medium this molecule readily precipitates and does not suffer from further additions of a proton to give $(\text{Co}_2)\text{H}$.

As commented above, the stability of the organocuprous intermediate during the decarboxylation reaction determines if the reaction occurs. The stability of the organocuprous is determined by a favorable interaction between cuprous ion and the decarboxylated residue. In the case of cyanoacetic acid, a molecule which quantitatively decarboxylates in the presence of a Cu(I) salt, it has been proposed that the organocuprous intermediate is stabilized by the interaction of the cyano π system with the Cu(I) ion.⁴⁴ In the case of $\text{Cu}_3\{\mu_2\text{-}(\text{Co}_2)\}_3$, it is clear that the reaction is driven by the stability of this molecule, as shown by the computed total bonding energy between the Cu_3^{3+} and $\{(\text{Co}_2)\}_3^{3-}$, which is as large as the corresponding one computed for $\text{Cu}_3(\mu_2\text{-CH}_3)_3$ (see above and Tables 4 and 5).

Conclusions

We have obtained a new Cu(I) bridged triangular cluster; $\text{Cu}_3\{\mu_2\text{-}(\text{Co}_2)\}_3$, which is a reaction product of copper(II) methoxide and Co_2COOH . The decarboxylation reaction of organic carboxylic acids is catalyzed by Cu(I), and the process is favored by a stable copper(I) organometallic intermediate. In our system it is clear that the organometallic copper(I) intermediary is stable enough to be isolated in the solid state. This particular stability of the compound, which is in the last term the driving force for the reaction, is determined by a strong interaction of the central copper(I) core and the peripheric bridging organocobalt fragment. A significant part of this interaction is accounted in terms of π interactions as shown by DFT calculations.

- (39) Calvo-Pérez, V. Ph.D. Thesis, University of Notre-Dame, 1995.
 (40) Darensbourg, D. J.; Holtcamp, M. W.; Khandelwal, B.; Reibenspies, J. H. *Inorg. Chem.* **1994**, *33*, 531.
 (41) Toussaint, O.; Capdevielle, P.; Maumy, M. *Tetrahedron Lett.* **1987**, *28*, 539.
 (42) Darensbourg, D. J.; Longridge, E. M.; Atnip, E. V.; Reibenspies, J. H. *Inorg. Chem.* **1992**, *31*, 3951.
 (43) Darensbourg, D. J.; Longridge, E. M.; Holtcamp, M. W.; Klausmeyer, K. K.; Reibenspies, J. H. *J. Am. Chem. Soc.* **1993**, *115*, 8839.
 (44) Darensbourg, D. J.; Longridge, E. M.; Atnip, E. V.; Reibenspies, J. H. *Inorg. Chem.* **1991**, *30*, 358.

Acknowledgment. The authors acknowledge financial support of FONDECYT (Grants 1980896, 2990093, and 4000027), FONDAP (Grant 11980002), and the French-Chilean CNRS/CONICYT program (PICS 922).

Note Added after ASAP: In the version of this paper posted ASAP on June 4, 2002, the first names and family names of some of the authors of refs 27, 30, and 32 were

interchanged. The correct author names appear in the version posted on June 12, 2002.

Supporting Information Available: XPS spectrum and X-ray data in CIF format for $\text{Cu}_3\{\mu_2\text{-(CO}_2)\}_3$. This material is available free of charge via the Internet at <http://pubs.acs.org>.

IC020117J